УДК 624.143.3 DOI 10.55421/3034-4689_2025_28_10_56

D. A. Diakite, A. A. Novikov

RECENT PROGRESS IN IMPROVING THE RESISTANCE OF SUPERHYDROPHOBIC SURFACES TO ICING

Keywords: icing, deicing, anti-icing, superhydrophobic surface, preparation methods.

Ice formation on solid surfaces negatively impacts many commercial and residential activities. Infrastructure and equipment surfaces covered with ice and frost can pose safety risks for road, aviation, maritime, and electric transport, as well as pedestrian safety. Superhydrophobic coatings have attracted increasing interest for their water-repellent properties in combating icing, but their practical application is limited by low abrasion wear resistance, poor adhesion to substrate, and insufficient chemical stability. Current research focuses on improving the effectiveness of de-icing and anti-icing methods and understanding the factors influencing frost formation to reduce icing-related risks to infrastructure and human safety. This review article presents the main mechanisms for preventing ice formation and recent advances in the preparation of superhydrophobic anti-icing surfaces. The main methods of stenciling, sputtering, immersion, chemical vapor deposition, layer-by-layer deposition, electrodeposition and etching are examined. Current results on the application of wear-resistant, self-healing, and electrothermal superhydrophobic coatings and related technologies in the field of deicing and anti-icing are discussed, along with future research directions.

Д. А. Диаките, А. А. Новиков

ПОСЛЕДНИЕ ДОСТИЖЕНИЯ В ОБЛАСТИ УЛУЧШЕНИЯ УСТОЙЧИВОСТИ СУПЕРГИДРОФОБНЫХ ПОВЕРХНОСТЕЙ К ОБЛЕДЕНЕНИЮ

Ключевые слова: обледенение, оттаивание, антиобледенение, супергидрофобная поверхность, методы подготовки.

Образование льда на твердых поверхностях негативно влияет на многие виды коммерческой и бытовой деятельности. Оно связано с фазовыми переходами воды, которые зависят от температуры и влажности окружающей среды. В условиях низких температур и высокой влажности происходит конденсация водяного пара, что приводит к образованию инея и льда на твердых поверхностях. Поверхности инфраструктуры и оборудования, покрытые льдом и инеем, могут представлять риск для безопасности дорожного движения, авиации, морского транспорта и электромобилей, а также безопасности пешеходов. Дороги и мосты, покрытые льдом, становятся скользкими и неустойчивыми, что увеличивает риск аварий и повреждений. Лед и иней на взлетно-посадочных полосах аэропортов могут привести к задержкам и отменам рейсов, а также увеличить риск аварий при посадке и взлете воздушных судов. Это явление требует детального анализа и разработки эффективных мер по его предотвращению и минимизации его последствий. Супергидрофобные покрытия привлекают все больший интерес своими водоотталкивающими свойствами в борьбе с обледенением, но их практическое применение ограничено низкой стойкостью к абразивному износу, а также недостаточными адгезией к подложке и химической стабильностью. Текущие исследования сосредоточены на повышении эффективности методов удаления льда и защиты от обледенения и понимании факторов, влияющих на образование инея, для снижения рисков, связанных с обледенением, для инфраструктуры и безопасности человека. В этой обзорной статье представлены основные механизмы предотвращения образования льда и последние достижения в подготовке супергидрофобных антиобледенительных поверхностей. Рассматриваются основные методы трафаретной печати, напыления, погружения, химического осаждения из паровой фазы, послойного осаждения, электроосаждения и травления. Обсуждаются текущие результаты по применению износостойких, самовосстанавливающихся и электротермических супергидрофобных покрытий и связанных с ними технологий в области борьбы с обледенением и защиты от обледенения, а также будущие направления исследований.

1. Introduction

The phenomenon of icing occurs when water in the liquid or gaseous state turns into solid ice on a surface, generally at a temperature below 0 °C. The adhesion of ice to solid surfaces has significant consequences for various sectors, including aviation, road transport, offshore platforms, supply vessels, wind turbines and power lines, as well as human safety [1–5]. Ice formation changes the shape of the wings, causing a loss of lift and compromising the aircraft's ability to fly. It increases drag and can change the aircraft's stall angle, making control more difficult and potentially dangerous [6]. The accumulation of ice, especially in winter, can lead to significant problems and damage frozen structures. It can cause damage to roofs, gutters and patios, as well as underground infrastructure, such as pipelines. Ice can also increase the risk of falls and injuries. Frequent removal of ice can lead to increased damage due to the strong adhesion of ice to most materials. To overcome this problem, researchers and scientists have developed innovative approaches to creating surfaces with modified adhesion characteristics. In particular, materials with reduced adhesion to ice structures have been designed and manufactured to minimize the negative effects of icing and to increase the resistance of structures to low temperatures [7,8].

The methods used in icing control can be classified into active and passive methods. Active deicing involves the use of external energy to break the ice layer. These include electrothermal deicing, which uses electric current to heat the surface, mechanical deicing, which involves physical action on the ice, and chemical deicing, which relies on the use of reagents to lower the freezing point of water. Despite the development of effective deicing and anti-icing technologies, they are characterized by high energy consumption, high

operating costs, potential damage to material surfaces, and are environmentally unfriendly [9]. Therefore, there is a need to study materials related to anti-icing and anti-ice control technologies in various fields, including domestic, industrial, economic, and construction sectors. Passive anti-icing surface treatments involve chemical or physical modification of the material surface. These methods promote rapid separation of water droplets from the base, which significantly reduces the risk of ice formation. In addition, these technologies significantly reduce the adhesion of ice to the surface, further increasing the effectiveness of anti-icing protection.

Fig. 1 - Superhydrophobic lotus leaf surface [9]

Inspired by the phenomenon of superhydrophobicity observed in nature (Fig. 1), for example in the self-cleaning ability of lotus leaves and the effect of the "anti-water" legs of a water strider, researchers have developed innovative artificial surfaces with a high degree of hydrophobicity [10]. These materials exhibit exceptional characteristics that open up broad prospects for applications in various branches of science and technology. In the study of surface properties, researchers have paid special attention to surfaces with a contact angle greater than 150° and a contact hysteresis angle less than 10° and they are designated as superhydrophobic surfaces [11–14]. These properties are due to a specific geometry that minimizes the contact area with the liquid, thus reducing surface tension and promoting self-cleaning of the surface. Hydrophobic and superhydrophobic materials are resistant to water, corrosion, biofouling and pollution, making them highly demanded in the technological field [15,16].

This article analyzes the mechanisms to inhibit the formation and growth of ice on the surfaces of superhydrophobic (SH) materials. Three key characteristics of SH materials are discussed: the elimination of water droplets before freezing, the control of the formation of ice crusts and the reduction of ice adhesion. The different methods of creating SH surfaces and their applications in various fields are examined. Finally, we review recent advances in research on SH materials for protection against icing.

2. Superhydrophobic de-icing and anti-icing mechanism

The discovery of the superhydrophobic characteristics of some animals and plants in nature has allowed researchers to mimic them and prepare SH materials with micro/nanostructures. The developed superhydrophobic surfaces can be effective for anti-icing and de-icing due to their ability to repel water and reduce ice adhesion. They achieve this through micro-nanostructures that trap air, minimizing contact between the surface and water, thus delaying ice formation (anti-icing) and promoting its removal (de-icing). There are three basic principles of ice prevention on SH surfaces (as shown in Figure 2) which are reducing the residence time of water droplets so that they do not freeze, slowing down the freezing of the drops, and reducing ice adhesion even when the droplets freeze [17–20].

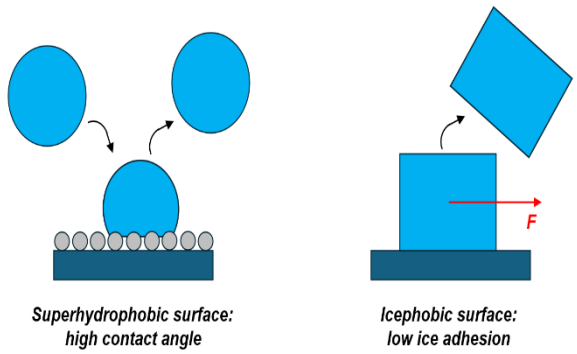

Fig. 2 - Schematic diagram of the anti-icing theory of superhydrophobic coatings [21]

2.1. Reduction of contact time of water droplets with superhydrophobic surfaces

Superhydrophobic coatings, characterized by a water contact angle greater than 150° and a rolling angle less than 10°, allow water droplets to slide easily. These materials provide water-repellent, anti-corrosion, bioresistant, and contaminant-resistant properties, while facilitating liquid flow. Analysis of previous studies demonstrates that superhydrophobic materials exhibit high efficiency in inhibiting the freezing process of aqueous droplets [22]. A water droplet on a superhydrophobic surface forms a Cassie-Baxter pattern, thus reducing interaction with the surface [23]. When the droplet is tilted, it slides on the surface [24]. Contact angle hysteresis significantly affects ice adhesion and growth on superhydrophobic surfaces under dynamic flow conditions [25]. Low contact angle hysteresis (CAH) generally delays ice formation and reduces adhesion, while higher hysteresis promotes its accumulation. The dynamic behavior of droplets impacting these surfaces, influenced by hysteresis, plays a crucial role in determining icephobic properties. Water droplets on the SH surface contract and rebound due to the low CAH [26], which allows their removal before/during freezing [27]. In practice, drops fall at different angles, with different heights and kinetic energy. They expand, deform, contract, and rebound from the SH surface.

In [28], the icephobic properties of SH surfaces are investigated using a wind tunnel at a temperature of -7 °C and a flow rate of 12 m/s. The coatings were applied to aluminum and steel plates. Monitoring was carried out

using CCD cameras. The results show that superhydrophobic coatings significantly slow down ice formation and accumulation, especially with low contact angle hysteresis and high roughness. This highlights the importance of a non-wetting state with low hysteresis, not just a high static contact angle.

Current methods for contact time reduction focus on engineering superhydrophobic surfaces with secondary, macroscopic or nanoscopic textures, or on designing specific nanotextures. The authors [29] present a simple and effective approach of replacing perfluorosilane (PFOS) coatings with liquid perfluorinated polyether (PFPE). Although their apparent contact angles are similar, PFPE-coated surfaces exhibit a 26% reduction in contact time compared to PFOS-coated surfaces due to an increased retraction speed. Surprisingly, while a conventional inertial model predicts only a 3% difference, PFPE surfaces exhibit a 12–32% reduction in retraction time. This improvement is attributed to lower contact angle hysteresis and increased interface slip on the liquid coating.

2.2. Delay icing

To understand the resistance of superhydrophobic surfaces to icing, it is essential to understand the icing mechanism. Water freezing is a very common phenomenon in nature. In essence, the freezing of water droplets is a liquid-to-solid phase transition, triggered by the nucleation (formation of the first ice crystals) of the new phase within the water droplets and their growth into three-dimensional ice crystals. Liquid water, even at temperatures below 0°C (supercooled water), can remain liquid until an ice «nucleus» form. This nucleus can be a dust particle, a surface imperfection, or an existing ice crystal. Once the nucleus forms, the surrounding water molecules arrange themselves around this nucleus, forming a three-dimensional ice crystal. This growth process continues as long as conditions (temperature, presence of liquid water) allow it. Indeed, delaying the freezing period implies an increase in the time needed for ice to begin to form (nucleation). Nucleation requires some time for water molecules to reach a sufficiently ordered state, which involves overcoming an energy barrier (interface between ice and liquid water) [30]. Superhydrophobic coatings, with micro-nanometer roughness, allow air pockets to be trapped under the droplets, resulting in the formation of a Cassie-Baxter wetting pattern. The trapped air creates an effective thermal insulation layer that prevents heat exchange with the substrate and prevents the droplets from freezing, thus delaying the icing process [31,32]. Superhydrophobic surfaces have higher surface roughness and low surface free energy. This increases the static contact angle (>150) and reduces the adhesion force of ice, which slows down surface freezing [33].

2.3. Reduction of ice adhesion to solid surfaces

Ice adhesion is one of the parameters for evaluating the anti-icing performance of a superhydrophobic material [34]. Indeed, the weaker the ice adhesion, the easier it will be to remove the formed ice, which is the main objective of anti-icing coatings to ensure the safety and functionality of various infrastructures in low temperature conditions. The reduction of ice adhesion force leads to its removal from the surface under the effect of its own weight or external forces (wind, gravity, vibration, etc.) [35,36]. Ice adhesion force and water contact angle are inversely correlated at the nanoscale, which means that superhydrophobic surfaces with a high-water contact angle and low hysteresis tend to exhibit lower ice adhesion force. Rønneberg et al. [37] used molecular dynamics to study this connection on the graphene surface. The results confirmed the theoretical predictions, taking into account material deformations and experimental factors.

Brassard et al. [38] electrodeposited thin zinc films onto steel substrates and functionalized them with superthin layers of silicone rubber to achieve superhydrophobic properties. Scanning electron microscopy (SEM) showed the micro/nano rough structure of the films, and X-ray diffraction and infrared spectroscopy confirmed their chemical composition. The optimal electrodeposition conditions (electric potential and time) provided a water contact angle of 155±10, which is important for corrosion and ice protection in marine conditions. The corrosion resistance of the coated steel was higher than that of the bare steel, and the ice adhesion strength decreased by 6.3 times.

The strong adhesion of ice to solid materials is due to strong intermolecular interactions between (polar) ice molecules and atoms/molecules of the solid material. These interactions are mainly hydrogen bonds, van der Waals forces, mechanical force and electrostatic interactions [23,39]. Electrostatic interactions contribute to adhesion by creating attractive forces between the charged surfaces of the ice and the substrate. To reduce adhesion, it is therefore necessary to decrease the electrostatic interaction between the ice molecules and the surface molecules.

The effectiveness of SH surfaces in reducing ice adhesion has been debated, with conflicting results among research groups. While some studies show that SH surfaces can reduce ice adhesion, others report increased adhesion. This variability is explained by the lack of a standardized ice adhesion test and the diversity of methodologies employed by researchers. Therefore, further research is important to better understand and improve the fundamental theory of the anti-icing properties of superhydrophobic materials.

3. Methods of preparation superhydrophobic surfaces

The key factors for creating superhydrophobic surfaces are chemical composition and roughness. Researchers have adopted two main approaches: (i) creating roughness on low surface energy materials (silicones, fluorocarbons, long-chain fatty acids) and (ii) modifying a rough surface with low surface energy materials [40,41]. For hydrophilic materials, roughness is first created, and then a low surface energy material is applied. The main reactive molecules to be modified are long-chain alkyl thiols, organic silanes, perfluorinated agents, fatty acids, PDMS-based polymers, and their combinations. Methods for roughness creation and modification include templating, etching, hydrothermal

synthesis, anodizing, electrodeposition, sol-gel, nanocomposite coating, and sputtering [42,43].

3.1. Template method (modeling)

Superhydrophobic surface preparation methods that use a master template to create specific structures on the material can be divided into two main groups: those using polymer templates and those using metal templates [17,44]. These templates act as matrices or molds to transfer their shape and topography to the surface of the final material, creating the roughness necessary to achieve superhydrophobic properties. Polymer templates are usually made from polymers such as polytetrafluoroethylene (PTFE), polypropylene (PP), and polydimethylsiloxane (PDMS), which can be easily molded and reproduced. They are often used for small-scale applications due to their flexibility and ease of handling. Metal (steel, aluminum) or glass templates offer greater durability and heat resistance. They are often used for the production of superhydrophobic surfaces on a large scale. The template method is a widely used technique in the preparation of polymer surfaces due to its simplicity, speed, and ability to reproduce complex textures from natural surfaces. Its main advantage lies in the ability to create surfaces with controlled properties, mimicking biological structures or other surfaces with specific patterns.

In [45], silica particles were coated onto cotton fibers, followed by coating FAS and FA-PEG molecules onto a silicon dioxide-coated fabric. FAS binds to silica via silanol groups and to cotton via hydroxyl groups. FA-MEG-PA is immobilized by interaction with FAS. All components adhere tightly to the fibers to form a stable layer. FAS molecules are integrated into the layer by self-bonding and interactions between fluorinated alkyl chains (Figure 3a). The PEG-phosphate groups on the coating surface were partially aggregated, making the sites hydrophilic. The fluorinated alkyl groups were also exposed due to the embedded FAS, which increased the dry oil repellency. The rough surface of the silica nanoparticles and the texture of the fabric further increased the oil repellency. The combination of hydrophilic and oleophobic sites with roughness resulted in superhydrophilicity and superoleophobicity (Figure 3b).

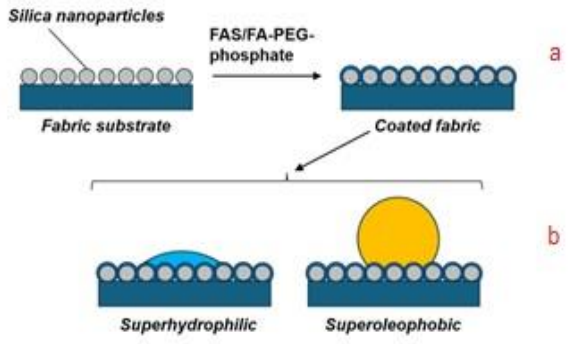

Fig. 3 - The coating mechanism: (a) the structure of the coating on cotton, (b) the wetting properties of the coated fabric [45]

In a study of creating transparent superhydrophobic coatings with sufficient mechanical strength, the authors [46] used methylacryloxypropyltrimethoxysilane (MEMO) polymerized into PMEMO to improve strength. Hydrophobic SiO_2 nanoparticles were fixed in the PMEMO mesh to prevent agglomeration. After coating PMEMO/SiO_2 on the glass slide, the light transmission rate was 89.24%. The coating retained its superhydrophobic properties when exposed to 160 g sand and a water jet at a speed of 4.6 m/s for 360 seconds, as well as after heat treatment at a temperature below 200°C.

A polyaniline (PANI) surface with biomimetic superhydrophobic structures was first obtained by nanocasting and used for corrosion protection [47]. PANI was synthesized by oxidative polymerization of aniline with ammonium persulfate in 1.0 M HCl. Then, superhydrophobic PANI were fabricated using PDMS and a cold-rolled steel electrode. The contact angle of water with the surface increased from 90° to 156°. Electrochemical tests showed that superhydrophobic PANI provides better corrosion protection than conventional PANI.

3.2. Coating methods

Coating methods involve applying a layer of material to a surface to modify its properties or appearance. These methods can be classified into liquid (solution) and solid (powder or nanoparticles) processes [48]. Coating methods can be subdivided into various techniques such as spraying, dipping, vapor deposition, centrifugation, etc.

3.2.1. Spray coating

Spray coating is one of the most widely used surface treatment techniques. It is based on atomizing coating materials and spraying them onto a surface, providing a protective or functional layer. There are different types of spray coatings, including thermal spraying [49], cathodic sputtering [50] and paint spraying [51].

Superhydrophobic materials are attracting great interest due to their applications in self-cleaning and liquid separation. Cao et al. [52] developed a method for creating hybrid PDMS/TiO_2 fibers for superhydrophobic coatings with a contact angle of up to 155°. These coatings are self-cleaning, corrosion-resistant, and durable. They are also effective for gravity separation of oil and water, as well as for filtering corrosive solutions, including salts, acids, and alkalis. Xu et al. [53] fabricated a superhydrophobic metal mesh by spraying metal salts and alkantiols to reduce surface energy and improve roughness. The maximum load-bearing capacity is achieved at a pore size of 90 μm. The mesh is stable and corrosion-resistant in pH 1–13 solutions. The superhydrophobic coating reduces the bias current by two orders of magnitude by protecting the substrate.

Non-fluorinated treatment developed for superhydrophobic textiles with durability and comfort [54]. The treatment includes two sprays: 1 - silica nanoparticles (214 nm) in ethanol and water (75/25), stabilized by an ammonia catalyst; 2 - a mixture of reactive polydimethylsiloxane and alkylsilane optimized by the RSM method. The water contact angle is 157°, which is maintained after 15 washes. To improve wear resistance, 3-aminopropyltrimethoxysilane (APS) is added, which maintains the angle at 5° after 1000 rubbing cycles. The air permeability of the treated textiles was 26.4 mL/(s cm²), creases and recovery after folding

remain unchanged, denoting durable water repellency that preserves physical comfort properties.

3.2.2. Dip coating

Dip coating is used to apply a variety of coatings, such as paints, varnishes, metals, or polymers, on different types of materials. The different types of immersion coatings can be formed by immersion in a powder bath (fluidized bed), by immersion in a liquid solution and by immersion in a molten metal bath (hot galvanization). The immersion coating process usually involves the following steps: substrate preparation, immersion, removal, drainage and drying followed by curing. The substrate intended for the coating is immersed in the original solution and then extracted at a constant removal rate. The process is carried out at strictly controlled temperatures and environmental parameters. A careful adjustment of the film properties, such as thickness, optical characteristics and internal structure, is achieved by precisely controlling the shrinkage speed and evaporation conditions. The uniform distribution of the solution on the surface of the substrate is ensured by the joint action of the viscous resistance and the capillary forces. The final stage of the process involves evaporation, which hardens the formed film. After coating, the substrates are often heat treated, which affects their operating properties [55]. The effectiveness of the immersion coating depends on the pH, the concentration and the viscosity of the solution. More viscous solutions require fewer repetitions to achieve the desired thickness, but can lead to bonding [56]. Less viscous solutions ensure uniformity repeatedly. The immersion rate could also affect the coating result.

Butt et al. [57] presented an innovative and cost-effective photonic platform based on silicon dioxide and titanium oxide, grown by sol-gel immersion using prisms. The analysis of the modal sensitivity of the waveguide is performed by the finite element method. Waveguides made from these materials are attractive due to their simplicity, low cost, low loss, and operation in the visible and near-infrared range. Simulations of the ring resonator sensor to determine the refractive index showed a sensitivity of 230 nm/RIU, a figure of merit (FOM) of 418.2 RIU^{-1}, and a Q factor of 2247.5 with improved geometric parameters.

Bouacheria et al. [58] prepared the thin films of pure zinc oxide (ZnO) and its aluminum (Al) doped variant (0.5, 1, 1.5 and 3 at.%) on glass substrates by dip coating with Zn and Al precursors. Their properties were studied using XRD, SEM, EDS, AFM, UV-Vis, PL and four-point probe. X-ray analysis revealed the polycrystalline nature of the films with c-axis (002) orientation and a decrease in the average crystallite size (29-25 nm) with an increase in Al concentration. EDS confirmed the presence of Zn, O and Al. Optical measurements showed the transparency of ZnO (up to 90 %) and the band gap of 3.16-3.26 eV. SEM revealed a wrinkled morphology that changed with increasing Al. The PLs showed high emission intensity (except for the film with 1 at. % Al), making them promising for solar cells.

3.2.3. Spin coating

Spin coating is a simple and widely used method for depositing thin films on flat substrates. The principle involves depositing a small amount of liquid (the coating material) in the center of the substrate and then rotating it at a controlled high speed (fig. 4). The resulting centrifugal force spreads the liquid evenly into a thin layer from the center to the edges of the substrate surface, which can then be solidified by solvent evaporation or other processes. This method is used in many applications, including the manufacture of semiconductors, optical devices, and nanomaterials. TiO_2 is a popular photocatalyst with limited light absorption capacity in the ultraviolet band (3-5 % of the solar spectrum) due to the wide band gap (3.2 eV). Doping can reduce the band gap, but the additives cause defects that reduce the solar energy conversion efficiency. Researchers have developed a doping-free method. Priyalakshmi Devi et al. [59] for the first time obtained pure nanocrystalline TiO2 with a band gap up to 2.68 eV without dopants. The technique involved using sol-gel spin-coating technology for the fabrication of nanocrystalline thin films of anatase TiO_2. The films were annealed at 400-550 °C and studied by X-ray diffraction, Raman spectroscopy, UV-visible spectroscopy, FESEM, AFM. Arifin et al. [60] studied the influence of sol-gel spin coating speed on the spreading of the coating layer on material surfaces. The rotation speed of sol-gel spin coating affects the properties of n-TiO_2/ZnO double-layer thin film for solar cells. The study revealed that the optimum speed is 3000 rpm, providing a homogeneous and compact morphology with a uniform distribution of ZnO grains. Characterized by the presence of TiO_2 and ZnO peaks, with a predominance of the (002) ZnO plane, indicating high crystallinity. The optical transmittance reaches 75 % and the film energy is 3.10 eV. Thus, the rotation speed is essential to improve the film properties.

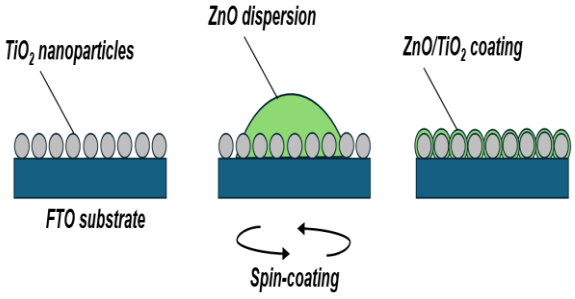

Fig. 4 - Illustration of the spin-coating process of a thin n-TiO_2/ZnO bilayer deposited on a fluorine-doped tin oxide (FTO) glass substrate [60]

Coating materials for electronic and optical devices have been studied for their unique properties. The ideal material should be highly transparent, superhydrophobic, strong, and durable. Ji et al. [61] designed and developed a strong and durable organic/inorganic hybrid coating without compromising transparency and hydrophobicity from handcrafted resin and hydrophobic silica nanoparticles by sol-gel spin-coating technology with high transparency (93.6 %), superhydrophobicity (CA: 160.1 ± 1°, SA: 7 ± 1°, σ2: 0.862), mechanical strength (CA maintained at 140° after 200 cycles), and resistance to acids, UV, water, and heat.

3.2.4. Layer-by-Layer (LbL) method

Thin film application technologies are essential for the development of functional materials in demand in various fields. The layer-by-layer (LbL) method is a thin film fabrication technology in which materials with opposite charges are adsorbed in series onto a substrate. Between each adsorption step, washing is performed to remove unadsorbed components. This approach ensures high precision in tuning the thickness and composition of the films. Over the last half century, there has been considerable and growing interest in the method of layer-by-layer assembly of nanoscale films [62]. LBL methods not only determine the key characteristics of the synthesis process but also have a direct impact on the morphological and functional properties of the formed films [63].

The layered nanofiltration (NF) membrane was obtained by inkjet printing of polyethylene (PEI) and graphene oxide (GO) on a polyketone (PK) membrane followed by glutaraldehyde (GA) crosslinking [64]. The characteristics of the membranes were confirmed by FTIR and SEM. The three-layer (PEI/GO)3 membrane showed optimal properties with high permeability and selectivity. The (PEI/GO)3 membrane exhibited a rejection performance of 99.9 %, 98.1 %, 94.7 %, and 85.1 % for Rose Bengal (RB), Brilliant Blue R 250 (BBR), Eosin Y (EY), and Methyl Blue (MB), respectively, and a selectivity for salts in the following order: $MgSO_4 > Na_2SO_4 > MgCl_2 > NaCl$. PEI and GO concentrations affect membrane performance. The (PEI/GO)3 membrane remained stable over the long term during chlorination and filtration. The results open up prospects for the production of stable LBL membranes with good NF properties.

3.2.5. Electrochemical deposition method

Electrochemical deposition, or electrodeposition, is a technique for forming thin films and nanostructures on conductive substrates by performing electrochemical reactions. The process involves supplying an electric current to a solution containing the ions of the deposited material, which causes their reduction and deposition on the substrate. Regulation of parameters such as voltage, current, and concentration of reactants allows the morphology and growth rate of crystals to be controlled [17]. Jiang et al. [65] developed a method to produce binder-free multilayered metallic mesoporous films for high electrocatalytic activity. Using a programmed electrochemical strategy, it is possible to synthesize structures with alternating mesoporous layers of Pd and PdPt of controlled thickness in a single electrolyte with polymer micelles. This architecture, combining the advantages of bimetallic alloys, multilayered and mesoporous structures, exhibits high activity in methanol oxidation (MOR) and ethanol oxidation (EOR) reactions.

In [66], the authors created superhydrophobic surfaces with a nickel film on copper substrates by a one-step electrodeposition method. The water contact angle reaches 160.3 ± 1.5° with a low rolling angle of 3.0 ± 0.5°. Once coated, the copper surfaces become rough with a cauliflower-like texture, which traps air and prevents water from contacting the copper. The coating is composed of nickel crystals and nickel myristate. The corrosion resistance of the coating was tested by potentiodynamic polarization and electrochemical impedance spectroscopy. The results show excellent corrosion inhibition in seawater.

3.2.6. Chemical vapor deposition

Chemical vapor deposition (CVD) is a technique in which a solid material is applied to a substrate by chemical reactions between gaseous reactants at elevated temperatures to form a thin film. This process involves introducing reactant gases into a chamber with a preheated substrate, where they interact with the surface to form a solid layer that is deposited on the substrate. CVD synthesis has reached new heights with the precise fabrication of inorganic thin films of 2D materials and high-purity polymer thin films that can be uniformly deposited on various substrates [67]. The process of chemical vapor deposition varies depending on the pressure, types of reactants, and reaction activation. CVD can also be performed in atomic layer deposition (ALD) mode to create multilayer structures. The advantages of CVD include the selective application of the material to specific areas of the substrate, which distinguishes it from physical vapor deposition.

To optimize industrial deposition processes in long and narrow tubes and channels, the authors [68] applied chromium carbide layers using liquid-injection metal-organic chemical vapor deposition in long (0.3-1 m) and narrow (8-24 mm) tubes. Bis(benzene)chromium (BBC) in toluene with N2 as carrier gas was used as a precursor. A multicomponent model is constructed to describe mass transfer, heat transfer, and chemical composition. The growth kinetics of the films was studied by precursor depletion experiments along the tube wall. The model operates at temperatures of 400-550 °C and pressures of 1,3x10□² à 7x10□³ Pa. The pressure affects the deposition rate and the uniformity of the coating thickness. At temperatures below 525 °C, the structure and composition of the films do not change. The coatings are amorphous with a Cr:C ratio of approximately 2:1. The model was used to design a long double-injection reactor to ensure coating uniformity and thickness.

Huang et al. [69] proposed a simple one-step method to create transparent superhydrophobic coatings with anti-wetting, self-cleaning, and anti-icing properties. Such coatings with networked nanocone structures are grown via initiated chemical vapor deposition (iCVD). The nanometer-sized monomers condense and form vertically aligned polymer nanocones with controlled height and density. The resulting coatings have improved water resistance, deicing properties, and light transmission compared to rough RC coatings. The frosting time reaches 540 s, which is 38.5 times and 2.2 times that of pristine glass and RC glass. The tests showed the durability and stability of the coating, making it promising for the protection of outdoor optoelectronic devices.

3.3. Etching method

Etching is a common method for creating superhydrophobic surfaces by texturing materials with micro- and nanostructures using laser, plasma, electrochemistry, and chemistry [9]. This technique allows creating a rough surface directly on a solid

material, thus minimizing the impact of adhesion between the coating and the substrate. The use of etching of metal surfaces is promising for creating micro-nanoscopic structures and obtaining superhydrophobic materials. The main advantage of this method is the integration of the formed superhydrophobic surface into the substrate structure, as well as its high corrosion resistance and stability of properties [70].

Laser-textured stainless-steel mesh loses its ability to separate oil and water after storage on air. This is due to the change in wettability due to metal oxides. To solve this problem, Ahlawat and his team [71] coated the metal mesh with a glass plate during laser processing. Coating the grid with a glass plate by laser plasma ablation creates a stable superhydrophilic/superoleophobic surface, retaining its properties for up to 8 months and ensuring oil and water separation with an efficiency of up to 96 %. The coated mesh is resistant to multiple abrasion cycles. Klimov et al. [72] studied the modification of the textured surface of aluminum by reactive copolymers of fluoroalkyl methacrylate with short-chain fluoroalkyl radicals and glycidyl methacrylate to obtain superhydrophobic properties. The obtained coatings exhibit contact angles up to 170° and recoil angles of 2–3°. The structure of the modified layer was examined by scanning electron microscopy and energy-dispersive X-ray spectroscopy. Wetting stability is improved due to repeated attachment of the modifier to the surface. Sun et al. [73] developed a method for creating a superhydrophobic aluminum alloy, combining high-speed EDM processing, short-term chemical etching, and modification processing. The sample has a contact angle of 158.6±1.3° and a sliding angle of less than 1°, which reduces the firing time from 20 to 8 hours. The alloy is resistant to mechanical damage, high (180-240 °C) and low temperatures, as well as abrasion and impact. The introduction of chemical etching improved the performance and durability of the material, expanding its application. The authors [74] described a method for creating nanoporous arrays on a polycarbonate substrate by trace etching. The films were irradiated with Ar^+ ions (220 MeV), UV irradiated, and etched in NaOH (2 N, 70 °C). The thickness of the matrices varied from 200 nm to several micrometers; the pore size varied from 15 to 100 nm. These matrices were successfully used to synthesize polypyrrole nanotubes and copper nanowires. The study of the morphology of the nanostructures was carried out by electron microscopy.

4. Recent advances in research on superhydrophobic surfaces

Research on superhydrophobic surfaces is progressing, particularly thanks to advances in texturizing and surface modification techniques. The creation and development of superhydrophobic anti-icing surfaces that delay ice formation and accumulation and reduce its adhesion is a key research area to address the problem of unwanted icing on the surfaces of critical structures [75]. Superhydrophobic surfaces, which repel water with very high efficiency, find applications in many fields, ranging from self-cleaning to corrosion and icing protection. However, practical applications of superhydrophobic surfaces are limited by the complexity of manufacturing processes, the brittleness of micro-nanostructured surfaces, high cost, low-temperature failure, poor mechanical durability, and pollution [76,77].

In recent years, researchers have actively developed and studied various approaches to solve the problem of low mechanical strength of superhydrophobic materials with anti-icing/de-icing effects. Anti-icing/de-icing coatings combining active and passive methods to improve the anti-icing performance of the substrate surface are used [78]. Recent advances in the field of wear-resistant, self-healing, photothermal, and electrothermal anti-icing superhydrophobic coatings are reviewed in this section.

To improve the durability and stability of superhydrophobic materials on aluminum alloy, an environmentally friendly method with boiling water and PDA@HDTMS nanocapsules is used [79]. The resulting surfaces have high strength, stability, excellent self-cleaning and corrosion resistance. An important advantage is self-healing, which opens new possibilities for improving the durability of materials. Sun et al. [80] proposed a laser processing method to create a superhydrophobic ultrafine brass wire that is promising in oil and water separation, anticorrosion, and deicing. The effects of laser power, scanning speed, and scanning time on morphology and wettability were analyzed. The superhydrophobic ultrafine brass wire exhibited the following optimal characteristics: 6 W laser power, 500 mm/s scanning speed, and 1 m scanning time. After processing, the water contact angle was 156°, and the roughness was 1.107 μm. Li et al. [81] presented a SiO_2/PDMS coating with FAS-17 on composite insulators by spraying. The coating has a contact angle of 159.2° and a sliding angle of 1.3°, thus improving the insulating properties. FAS-17-modified SiO_2 nanoparticles do not stick together. The binding energy is calculated using density functional theory, explaining the superhydrophobic mechanism. A new method has been proposed to solve the pollution problem of insulators and explain superhydrophobicity.

Liquid spraying of superhydrophobic coatings has advantages in terms of simplicity, low cost, and large-scale industrialization capability. However, these coatings suffer from insufficient wear resistance due to excessive or poor adhesion of nanoparticles. Liu's group [82] proposed a method to transform a continuous-phase adhesive into a discrete adhesive by separating the phases, which improves the wear resistance of the coatings by binding nanoparticles without scale formation. This approach is important for the practical application of superhydrophobic coatings.

The biochar-based deicing coating activated with copper sulfide (AC@Cars), hydrophobic polydimethylsiloxane, and thermosetting microspheres exhibits thermal insulation, superhydrophobicity, and photo/electrothermal effects [78]. This increases the freezing time of water droplets from 150 to 2140 seconds. With an electrical power density (EPD) of 0.2 W/cm^2 and an optical power density (OPD) of 0.1 W/cm^2, the coating temperature is increased to 96.4 and 113 °C, respectively. The coating effectively melts ice within 2.5 minutes with a combined heating of 0.05

W/cm^2. After mechanical damage, exposure to rain, UV, corrosion and high temperature treatment, the water contact angle of the prepared coating remains above 150 °C and superhydrophobicity ensures anti-/deicing durability of the coating.

Superhydrophobic surfaces with micro-nanostructures are effective in preventing icing but can be damaged during defrosting. Liu et al. [83] developed a low-adhesion superhydrophobic photothermal coating that self-regenerates under solar irradiation. The coating reaches a temperature of 85 °C, allowing ice to melt in 150 seconds. It has a contact angle of up to 162° and a tilt angle of up to 4.8°, which provides excellent anti-icing properties. The beeswax in the composition promotes self-healing of the coating after damage.

Conclusion

Superhydrophobic coatings protect against icing because water droplets can detach before freezing due to low surface energy, reduced contact area, and limited heat transfer. Their micro- and nanostructures reduce ice adhesion, making it easier to remove. However, superhydrophobic coatings can also enhance ice adhesion due to the anchoring effect. The characteristics of the coatings depend on the surface relief, but the microstructure is easily disrupted, which reduces their effectiveness. The preparation of superhydrophobic surfaces with excellent Cassie stability, minimal adhesion to icing, high resistance to corrosion, water, wear, and mechanical damage, and self-healing involves various modification methods, such as chemical vapor deposition (CVD), plasma spraying, dipping, and the use of nanotechnology to create textured layers. These methods allow to achieve high wetting contact angle values and ensure the durability of the coating under conditions of extreme temperatures and mechanical stress.

In recent years, researchers have made significant and innovative progress in developing wear-resistant and self-healing superhydrophobic coatings. These coatings not only have high hydrophobic properties but also resistance to mechanical damage, making them promising for applications in the aeronautical, automotive, and naval industries, etc. Self-healing coatings can restore their structure and properties after mechanical damage and exposure to corrosive environments. Low-energy approach techniques combining active deicing and passive anti-icing are proposed by researchers to increase the effectiveness of superhydrophobic surfaces in solving the icing problem. These are the techniques that apply superhydrophobic photothermal and electrothermal coatings that are promising in the field of icing management. Under the influence of light, photothermal coatings are activated, resulting in local heating and melting of the ice, while electrothermal coatings are activated under the influence of an electric current, which effectively removes ice and frost in hard-to-reach places.

Currently, most superhydrophobic coatings are produced on a laboratory scale. Therefore, it is necessary to conduct research and testing of these coatings in real-life conditions. Thus, research on superhydrophobic coatings opens up new possibilities for solving the problem of icing and freezing in various industries. The development and introduction of new anti-icing materials and technologies will improve the safety and efficiency of installations in conditions of low temperatures and high humidity.

References

1. Zhang, F., Yan, H., and Chen, M. *Small*, *20*,32, 2312226 (2024). DOI: 10.1002/smll.202312226.
2. Dehghani-Sanij, A.R., Dehghani, S.R., Naterer, G.F., and Muzychka, Y.S. Ocean Engineering *132*, 25–39 (2017). DOI: 10.1016/j.oceaneng.2017.01.016.
3. Shi, K., and Duan, X. Journal of Offshore Mechanics and Arctic Engineering *143, 6* (2021). DOI: 10.1115/1.4050893.
4. Huang, W., Huang, J., Guo, Z., and Liu, W. Adv Colloid Interface Sci *304*, 102658 (2022). https://doi.org/10.1016/j.cis.2022.102658.
5. Chen, J., Bai, X., Wang, J., Chen, G., and Zhang, T. Water *14, 23*, 3834 (2022). DOI: 10.3390/w14233834.
6. He, H., and Guo, Z. iScience *2, 11*, 103357 (2021). DOI: 10.1016/j.isci.2021.103357.
7. Gao, S., Liu, B., Peng, J., Zhu, K., Zhao, Y., Li, X., and Yuan, X.. *ACS applied materials & interfaces 11, 4*, 4654–4666 (2019). DOI: 10.1021/acsami.8b19666.
8. Mirshahidi, K., Alasvand Zarasvand, K., Luo, W., and Golovin, K. HardwareX *8*, e00146 (2020). DOI: 10.1016/j.ohx.2020.e00146.
9. Lin, Y., Chen, H., Wang, G., and Liu, A. Coatings *8, 6*, 208 (2018). DOI: 10.3390/coatings8060208.
10. Wang, L., Gong, Q., Zhan, S., Jiang, L., and Zheng, Y. *Advanced Materials*, *28*, 35, 7729-7735 (2016). DOI: 10.1002/adma.201602480.
11. Ellinas, K., Tserepi, A., and Gogolides, E. Advances in Colloid and Interface Science *250*, 132–157 (2017). DOI: 10.1016/j.cis.2017.09.003.
12. Teisala, H., and Butt, H.-J. Langmuir *35, 33*, 10689–10703 (2018).. DOI: 10.1021/acs.langmuir.8b03088.
13. Karapanagiotis, I. Coatings *13,3*, 551 (2023). DOI: 10.3390/coatings13030551.
14. Liu, W., Xiang, S., Liu, X., and Yang, B. ACS Nano *14, 7*, 9166–9175 (2020). DOI: 10.1021/acsnano.0c04670.
15. Vlasov, A.I., Mikhailov, A.V., Fedorenko, V.D., Novikov, A.A., Gorbachevskii, M.V., Kopitsyn, D.S., Vinokurov, V.A., Farahov, M.I., and Farahov, M.M. Neftyanoe khozyaystvo - Oil Industry *2019, 12*, 77–81 (2019). DOI: 10.24887/0028-2448-2019-12-77-81.
16. DIAKITE, D. A., and NOVIKOV, A. A. *Revue Internationale du Chercheur*, *6*, 2, 1247 1275 (2025). DOI: 10.5281/zenodo.15733137.
17. Cong, Q., Qin, X., Chen, T., Jin, J., Liu, C., and Wang, M. Materials (Basel) *16, 14*, 5151 (2023). DOI: 10.3390/ma16145151.
18. Maitra, T., Tiwari, M.K., Antonini, C., Schoch, P., Jung, S., Eberle, P., and Poulikakos, D. *Nano letters*, *14*, 1, 172-182 (2013). DOI: 10.1021/nl4037092.
19. Eberle, P., Tiwari, M.K., Maitra, T., and Poulikakos, D. *Nanoscale*, *6*, 9, 4874-4881 (2014). DOI: 10.1039/C3NR06644D.
20. Janjua, Z.A., Turnbull, B., Choy, K.-L., Pandis, C., Liu, J., Hou, X., and Choi, K.-S. Applied Surface Science *407*, 555–564 (2017). DOI: 10.1016/j.apsusc.2017.02.206.
21. Li, W., Zhan, Y., and Yu, S. Progress in Organic Coatings *152*, 106117 (2021). DOI: 10.1016/j.porgcoat.2020.106117.
22. Zhang, Y., Anim-Danso, E., Bekele, S., and Dhinojwala, A. *ACS applied materials & interfaces*, *8*, 27, 17583-17590 (2016).. DOI: 10.1021/acsami.6b02094.
23. Shen, Y., Wu, X., Tao, J., Zhu, C., Lai, Y., and Chen, Z. Progress in Materials Science *103*, 509–557 (2019).. DOI: 10.1016/j.pmatsci.2019.03.004.

24. Fan, Y., Tan, Y., Dou, Y., Huang, S., and Tian, X. Chemical Engineering Journal *476*, 146485 (2023).. DOI: 10.1016/j.cej.2023.146485.
25. Harvie, D. J. *Journal of Fluid Mechanics*, *986*, A17 (2024). DOI: 10.1017/jfm.2024.317.
26. Richard, D., Clanet, C., and Quéré, D. Nature *417,6891*, 811–811 (2002). DOI: 10.1038/417811a.
27. Gauthier, A., Symon, S., Clanet, C., and Quéré, D. Nat Commun 6*, 1*, 8001(2015). DOI: 10.1038/ncomms9001.
28. Sarshar, M.A., Swarctz, C., Hunter, S., Simpson, J., and Choi, C.-H. Colloid Polym Sci *291, 2*, 427–435 (2013). DOI: 10.1007/s00396-012-2753-4.
29. Fan, Y., Wu, C., Yang, J., Wang, Y., Zhou, Y., Zhou, J., Luo, J., Zhang, J., Huang, S., and Tian, X. Chemical Engineering Journal *448*, 137638 (2022). DOI: 10.1016/j.cej.2022.137638.
30. Alizadeh, A., Yamada, M., Li, R., Shang, W., Otta, S., Zhong, S., Ge, L., Dhinojwala, A., Conway, K.R., Bahadur, V., Vinciquerra, A.J., Stephens, B., and Blohm, M.L. Langmuir *28, 6*, 3180–3186 (2012). DOI: 10.1021/la2045256.
31. Shu, Y., Lu, X., Liang, Y., Su, W., Gao, W., Yao, J., Niu, Z., Lin, Y., and Xie, Y. Surface and Coatings Technology *441*, 128514 (2022). DOI: 10.1016/j.surfcoat.2022.128514.
32. Li, J., Zhou, Y., Wang, W., Xu, C., and Ren, L. Langmuir *36(5)*, 1075–1082 (2020). DOI: 10.1021/acs.langmuir.9b02273.
33. Wu, Y., Shen, Y., Tao, J., He, Z., Xie, Y., Chen, H., Jin, M., and Hou, W. New J. Chem. *42, 22*, 18208–18216 (2018). DOI: 10.1039/C8NJ04275F.
34. Zheng, H., Chang, S., Ma, G., and Wang, S. Energy and Buildings *223*, 110175 (2020). DOI: 10.1016/j.enbuild.2020.110175.
35. Bleszynski, M., and Clark, E. Standards *1, 2*, 117–133 (2021).. DOI: 10.3390/standards1020011.
36. Rønneberg, S., He, J., and Zhang, Z. Journal of Adhesion Science and Technology *34, 3*, 319–347 (2020). DOI: 10.1080/01694243.2019.1679523.
37. Rønneberg, S., Xiao, S., He, J., and Zhang, Z. Coatings *10, 4*, 379 (2020). DOI: 10.3390/coatings10040379.
38. Brassard, J.D., Sarkar, D.K., Perron, J., Audibert-Hayet, A., and Melot, D. Journal of Colloid and Interface Science *447*, 240–247 (2015). DOI: 10.1016/j.jcis.2014.11.076.
39. Jia, Z., Shen, Y., Tao, J., Zhang, Y., Chen, H., Lu, Y., and Wu, Z. Coatings *10, 11*, 1043 (2020). DOI:10.3390/coatings10111043.
40. Buijnsters, J.G., Zhong, R., Tsyntsaru, N., and Celis, J.-P. ACS applied materials & interfaces, *5, 8*, 3224–3233 (2013). DOI: 10.1021/am4001425.
41. Kim, S., Hwang, H.J., Cho, H., Choi, D., and Hwang, W. Chemical Engineering Journal *350*, 225–232 (2018). DOI: 10.1016/j.cej.2018.05.184.
42. Jiang, X., Zhuo, Y., Wang, P., Yang, M., Liao, Y., and Chen, B. Coatings *13, 2*, 326 (2023). DOI: 10.3390/coatings13020326.
43. Shan, L.-M., Liu, G.-B., Tang, H., Li, Z.-H., and Wu, J.-Y. Coatings *12, 11*, 1717 (2022). DOI: 10.3390/coatings12111717.
44. Maghsoudi, K., Vazirinasab, E., Momen, G., and Jafari, R. Ind. Eng. Chem. Res. *59, 20*, 9343–9363 (2020). DOI: 10.1021/acs.iecr.0c00508.
45. Zhou, H., Wang, H., Yang, W., Niu, H., Wei, X., Fu, S., Liu, S., Shao, H., and Lin, T. RSC Adv. *8, 47*, 26939–26947 (2018). DOI: 10.1039/C8RA04645J.
46. Wang, R., Hu, C., Li, J., Lin, X., and Zhang, W. ACS Appl. Polym. Mater. *5, 7*, 5230–5237 (2023). DOI: 10.1021/acsapm.3c00671.
47. Peng, C.-W., Chang, K.-C., Weng, C.-J., Lai, M.-C., Hsu, C.-H., Hsu, S.-C., Hsu, Y.-Y., Hung, W.-I., Wei, Y., and Yeh, J.-M. Electrochimica Acta *95*, 192–199 (2013). DOI: 10.1016/j.electacta.2013.02.016.
48. Butt, M.A. Coatings *12, 18*, 1115 (2022). DOI: 10.3390/coatings12081115.
49. Rezzoug, A., Gholenji, R.B., and Yandouzi, M. *Journal of Thermal Spray Technology*, 1-44 (2025). DOI: 10.1007/s11666-025-02023-2.
50. Zhai, M., Liu, Y., Huang, J., Hou, W., Wu, S., Zhang, B., and Li, H. J Therm Spray Tech *29, 5*, 1172–1182 (2020). DOI: 10.1007/s11666-020-01022-9.
51. Li, F., Lan, X., Wang, L., Kong, X., Xu, P., Tai, Y., Liu, G., and Shi, J. Chemical Engineering Journal *383*, 123092 (2020). DOI: 10.1016/j.cej.2019.123092.
52. Cao, K., Huang, X., and Pan, J. Polymers *14, 24*, 5431 (2022). https://doi.org/10.3390/polym14245431.
53. Xu, X.H., Zhang, Z.Z., Yang, J., and Zhu, X. Colloids and Surfaces A: Physicochemical and Engineering Aspects *377, 1-3*, 70–75 (2011). DOI: 10.1016/j.colsurfa.2010.12.024.
54. Mohseni, M., Far, H.S., Hasanzadeh, M., and Golovin, K. Progress in Organic Coatings *157*, 106319 (2021). DOI: 10.1016/j.porgcoat.2021.106319.
55. Montazerian, M., Baino, F., Fiume, E., Migneco, C., Alaghmandfard, A., Sedighi, O., DeCeanne, A.V., Wilkinson, C.J., and Mauro, J.C. Progress in Materials Science *132*, 101023 (2023). DOI: 10.1016/j.pmatsci.2022.101023.
56. Hakki, H.K., Allahyari, S., Rahemi, N., and Tasbihi, M. Chimie *22, 5*, 393–405 (2019). DOI: 10.1016/j.crci.2019.05.007.
57. Butt, M.A., Kaźmierczak, A., Tyszkiewicz, C., Karasiński, P., and Piramidowicz, R. Sensors *21, 22*, 7452 (2021). DOI: 10.3390/s21227452.
58. Bouacheria, M.A., Djelloul, A., Adnane, M., Larbah, Y., and Benharrat, L. J Inorg Organomet Polym *32, 7*, 2737–2747 (2022). DOI: 10.1007/s10904-022-02313-0.
59. Priyalakshmi Devi, K., Goswami, P., and Chaturvedi, H. Applied Surface Science *591*, 153226 (2022). DOI: 10.1016/j.apsusc.2022.153226.
60. Arifin, N.M., Mhd Noor, E.E., Mohamad, F., and Mohamad, N. Coatings *14, 1*, 73 (2024). DOI: 10.3390/coatings14010073.
61. Ji, Z., Liu, Y., and Du, F. Progress in Organic Coatings *157*, 106294 (2021). DOI: 10.1016/j.porgcoat.2021.106294.
62. Richardson, J.J., Cui, J., Björnmalm, M., Braunger, J.A., Ejima, H., and Caruso, F. *Chemical reviews*, *116*, 23, 14828-14867 (2016). DOI: 10.1021/acs.chemrev.6b00627.
63. Zhang, Z., Zeng, J., Groll, J., and Matsusaki, M. Biomater. Sci. *10, 15*, 4077–4094 (2022). DOI: 10.1039/D2BM00497F.
64. Wang, C., Park, M.J., Gonzales, R.R., Matsuyama, H., Drioli, E., and Shon, H.K. Desalination *549*, 116357 (2023). DOI: 10.1016/j.desal.2022.116357.
65. Jiang, B., Li, C., Qian, H., Hossain, M.S.A., Malgras, V., and Yamauchi, Y. Angew Chem Int Ed Engl *56, 1-7*, 7836–7841 (2017). DOI: 10.1002/anie.201703609.
66. Yang, Z., Liu, X., and Tian, Y. Colloids and Surfaces A: Physicochemical and Engineering Aspects *560*, 205–212 (2019). DOI: 10.1016/j.colsurfa.2018.10.024.
67. Sun, L., Yuan, G., Gao, L., Yang, J., Chhowalla, M., Gharahcheshmeh, M.H., Gleason, K.K., Choi, Y.S., Hong, B.H., and Liu, Z. Nat Rev Methods Primers *1, 1*, 5 (2021). DOI: 10.1038/s43586-020-00005-y.
68. Michau, A., Maury, F., Schuster, F., Nuta, I., Gazal, Y., Boichot, R., and Pons, M. Coatings *8, 6*, 220 (2018). DOI: 10.3390/coatings8060220.
69. Huang, X., Sun, M., Shi, X., Shao, J., Jin, M., Liu, W., Zhang, R., Huang, S., and Ye, Y. Chemical Engineering Journal *454*, 139981 (2023). DOI: 10.1016/j.cej.2022.139981.
70. Ge-Zhang, S., Yang, H., Ni, H., Mu, H., and Zhang, M. *Frontiers in Bioengineering and Biotechnology*, *10*, 958095 (2022). DOI: 10.3389/fbioe.2022.958095.

71. Ahlawat, S., Singh, A., Mukhopadhyay, P.K., Singh, R., and Bindra, K.S. Materials Chemistry and Physics *263*, 124343 (2021). DOI: 10.1016/j.matchemphys.2021.124343.
72. Klimov, V.V., Bryuzgin, E.V., Navrotskiy, A.V., and Novakov, I.A. Surfaces and Interfaces *25*, 101255 (2021). DOI: 10.1016/j.surfin.2021.101255.
73. Sun, R., Zhao, J., Li, Z., Qin, N., Mo, J., Pan, Y., and Luo, D. Progress in Organic Coatings *147*, 105745 (2020). DOI: 10.1016/j.porgcoat.2020.105745.
74. Dauginet-De Pra, L., Ferain, E., Legras, R., and Demoustier-Champagne, S. Nuclear Instruments and Methods in Physics Research Section B: Beam Interactions with Materials and Atoms *196, 1-2*, 81–88 (2002). DOI: 10.1016/S0168-583X(02)01252-1.
75. Wang, L., Zhao, H., Zhu, D., Yuan, L., Zhang, H., Fan, P., and Zhong, M. Applied Sciences *13, 9*, 5478 (2023). DOI: 10.3390/app13095478.
76. Zhang, J., Zhang, L., and Gong, X. Langmuir *37(19)*, 6042–6051 (2021). DOI: 10.1021/acs.langmuir.1c00706.
77. Erdene-Ochir, O., Do, V.-T., and Chun, D.-M. Polymer *255*, 125158 (2022). DOI: 10.1016/j.polymer.2022.125158.
78. Wei, H., Luo, H., Fan, W., Chen, Y., Xiang, J., and Fan, H. *ACS Applied Materials & Interfaces* 16, 27, 35613-35625 (2024). DOI: 10.1021/acsami.4c08289.
79. Zhang, Z., Xue, F., Bai, W., Shi, X., Liu, Y., and Feng, L. Surface and Coatings Technology *410*, 126952 (2021). DOI: /10.1016/j.surfcoat.2021.126952.
80. Sun, J., Huang, H., Ji, J., Zhang, C., Wu, B., Liu, H., and Song, J. Materials *18, 7*, 1420 (2025). DOI: 10.3390/ma18071420.
81. Li, C., Dou, P., Zhao, R., Shi, Y., Fu, G., and Shen, B. Coatings *13, 3*, 563 (2023). DOI: 10.3390/coatings13030563.
82. Liu, X., Shi, Z., Lin, L., Shang, X., Wang, J., Xie, C., and Wang, L. Coatings *13, 4*, 682 (2023). DOI: 10.3390/coatings13040682.
83. Liu, Z., Hu, J., and Jiang, G. Surface and Coatings Technology *444*, 128668 (2022). DOI: 10.1016/j.surfcoat.2022.128668.

© **D. A. Diakite**, Postgraduate student, Department of Physical and Colloid Chemistry, Faculty of Chemical Engineering and Ecology, Gubkin Russian State University of Oil and Gas, daoudaassadiakite@gmail.com; **A. A. Novikov**, Ph.D., Associate Professor, Department of Physical and Colloid Chemistry, Faculty of Chemical Engineering and Ecology, Gubkin, novikov.a@gubkin.ru.

© **Д. А. Диаките** – асп. кафедры физической и коллоидной химии, факультета химической технологии и экологии РГУ нефти и газа им. И.М. Губкина, : daoudaassadiakite@gmail.com№; **А. А. Новиков** - к.х.н., Доцент кафедры физической и коллоидной химии, факультета химической технологии и экологии РГУ нефти и газа им. И.М. Губкина, novikov.a@gubkin.ru.

Дата поступления рукописи в редакцию – 22.08.25.
Дата принятия рукописи в печать – 23.09.25.